Influence of casting temperature on microstructures and mechanical properties of $Cu_{50}Zr_{45.5}Ti_{2.5}Y_2$ metallic glass prepared using copper mold casting

Zhengwang Zhu
Shenyang National Laboratory for Materials Science, Institute of Metal Research, Chinese Academy of Sciences, Shenyang 110016, China; and Faculty of Engineering and Surveying, The University of Southern Queensland, Toowoomba, Queensland 4350, Australia

Haifeng Zhang[a)]
Shenyang National Laboratory for Materials Science, Institute of Metal Research, Chinese Academy of Sciences, Shenyang 110016, China

Hao Wang
Faculty of Engineering and Surveying, The University of Southern Queensland, Toowoomba, Queensland 4350, Australia

Bingzhe Ding and Zhuang-Qi Hu
Shenyang National Laboratory for Materials Science, Institute of Metal Research, Chinese Academy of Sciences, Shenyang 110016, China

Han Huang
Division of Mechanical Engineering, School of Engineering, The University of Queensland, Brisbane, Queensland 4072, Australia

(Received 17 March 2009; accepted 6 May 2009)

The influence of casting temperatures on microstructures and mechanical properties of rapidly solidified $Cu_{50}Zr_{45.5}Ti_{2.5}Y_2$ alloy was investigated. With increasing casting temperatures, the amount of the crystalline phase decreases. At a high casting temperature, i.e., 1723 K, glass-forming ability (GFA) of the present alloy is enhanced. The results imply that adjusting the casting temperature could be used for designing the microstructures of bulk metallic glass matrix composite. Nanoindentation tests indicated that CuZr phases are slightly softer and can accommodate more plastic deformation than the amorphous matrix. Compression tests confirmed that this kind of second phase (CuZr) precipitated under lower casting temperatures helps to initiate multiple shear bands, resulting in a great improvement in mechanical properties of the samples. Our work indicates that casting temperatures have a great influence on GFA, microstructures, and mechanical properties of the rapidly solidified alloy, therefore controlling the casting temperature is crucial to the production of BMGs.

I. INTRODUCTION

Properties of materials depend on their microstructures, while the microstructures are closely correlated to the manufacturing process used. Many processing methods, for example, quenching, annealing, cold working, etc., are developed to achieve the desired microstructures, further leading to obtaining the optimal properties.[1] Melt treatment, including ultrasonic vibration treatment,[2] superhigh temperature treatment,[3–5] etc., is evidenced to be effective in changing the microstructures and improving the properties of Al-, Ni-, and Fe-based alloys and have been widely used in industrial production.

Metallic glass (MG) has been developed for almost 50 years.[6] Similar to the steel industry, the database among processes, microstructures, and properties for bulk metallic glasses (BMGs) should be built up to promote their commercial applications.[7] In the past few decades, the researchers in this field have concentrated on developing alloy compositions with large glass-forming ability (GFA), in all common alloy systems, and understanding the relationship between microstructures and properties.[8–10] Some significant progress has been achieved as seen by the successful development of BMGs in many alloy systems, including Al, Fe, Ni, Cu, Zr, Mg, Re (rare-earth metals), etc., base alloys. The size of BMGs increasing from micrometer to inch[8–10] and the

[a)]Address all correspondence to this author.
e-mail: hfzhang@imr.ac.cn
DOI: 10.1557/JMR.2009.0373

plasticity of BMGs has been improved by introducing particle,[11] fiber,[12] etc., to form bulk metallic glass matrix composites (BMGCs). However, there are a few concerns on the relationship between processing techniques and properties of BMGs. Shen et al.[13] studied the effect of the cooling rate on plasticity of TiCu-based BMG. Manov et al.[3] and Popel et al.[4,5] reported the effect of quenching temperature on the microstructure of Al and Fe-based amorphous ribbons. In fact, the knowledge on this aspect must be setup because it is crucial to boost BMGs' applications. Our existing work has systematically studied the influence of the casting conditions on microstructures and properties of BMGs. In our two previous works,[14,15] we investigated the effect of casting temperatures on nanocrystal formation in the amorphous matrix and thermal stability of amorphous alloys. It is concluded that high casting temperature can effectively reduce the degree of heterogeneity in the alloy melts, leading to the enhancement of thermal stability and a decrease in plasticity in the resultant amorphous alloys. To extend these investigations, in this work, we concentrate on the influence of casting temperature on GFA. Furthermore, we discuss the relationship between the microstructures obtained under different casting temperatures and their mechanical properties.

II. EXPERIMENTAL

Cu-based BMGs were selected in this study because of low price and high strength along with the easy formation of in situ nanocrystals.[16–19] Ingots with nominal composition of $Cu_{50}Zr_{45.5}Ti_{2.5}Y_2$ were obtained by arc melting high purity elements under Ti-getter argon atmosphere. The amorphous ribbons with a thickness of about 60 μm were prepared by the single-roller melt-spinning method. The cylinder samples with different diameters were manufactured using the copper mold injection casting method under a high-purity argon atmosphere. The casting temperature (also called the quenching temperature in the melt spinning process) was monitored by an infrared thermoscope. Three casting temperatures were chosen, 1323, 1523, and 1723 K. The oxygen content of the samples fabricated under different temperatures was measured to be below 500 ppm. The continuous differential scanning calorimeter (DSC) experiment of amorphous ribbons was performed on a Netzsch DSC 204 (Selb, Germany) at a heating rate of 20 K/min. The apparatus was calibrated for temperature and enthalpy using highly pure indium and zinc before the measurements. Microstructures were checked using x-ray diffraction (XRD) (Cu K_α radiation; Philips PW1050, The Netherlands), optical microscopy and scanning electron microscopy (SEM; Hitachi S3400N, Tokyo, Japan). Compression tests (MTS 810, Eden Prairie, MN) and nanoindentation tests were performed to evaluate the mechanical properties of the samples. The fractured samples were also observed using SEM.

III. RESULTS

To check the influence of casting temperatures on glass formation in the $Cu_{50}Zr_{45.5}Ti_{2.5}Y_2$ alloy, the alloy was cast into 2 and 3-mm-diameter cylindrical samples under different casting temperatures of 1323, 1523, and 1723 K. Figure 1 shows their XRD patterns. Only the 2-mm-diameter samples prepared at 1723 K possess a broad peak in the XRD patterns, indicating that the sample is in the amorphous state. The other two 2-mm-diameter samples prepared at 1323 and 1523 K exhibit some Bragg peaks on the XRD patterns. For the samples with 3 mm diameter prepared at 1323, 1523, and 1723 K, the Bragg peaks are clearly seen in their XRD patterns, revealing that all 3-mm-diameter samples crystallized to some extent. The crystalline phases formed during solidification were indexed as CuZr, maybe a mixture of austenite and martensite phase (Powder Diffraction Data, International Center for Diffraction Data, published by JCPDS, Newton Square, PA, 2002). Furthermore, martensite transformation was confirmed in the DSC measurement (Fig. 2). Similar results were reported previously.[19–23] For 3-mm-diameter cast samples, we found that the percentage of the crystalline phase reduces with the increase of casting temperature, which is inferred from the intensity of Bragg peaks in the samples. This was further confirmed by DSC measurement and microstructure observation.

Figure 2 shows DSC curves of 2-mm-diameter samples prepared at different casting temperatures. The glass transition temperature, onset crystallization temperature, and crystallization enthalpy for these samples were determined, which are tabulated in Table I. In comparison, the ribbons prepared under 1323 and 1723 K were also

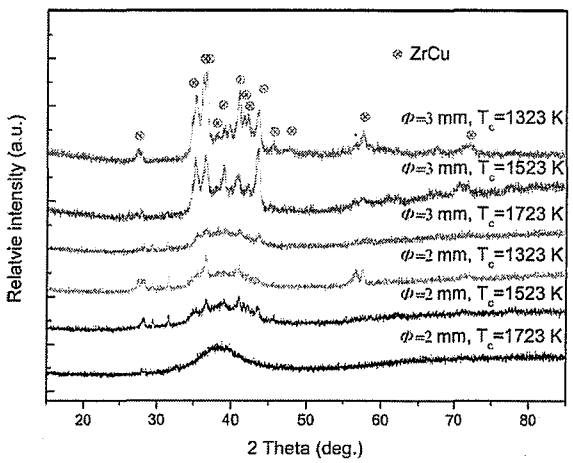

FIG. 1. XRD patterns of as-cast rods with different diameters and different casting temperatures in $Cu_{50}Zr_{45.5}Ti_{2.5}Y_2$ alloy.

measured, and the results were also listed in Fig. 2 and Table I. For the samples prepared under 1323 and 1523 K, some small endothermic peaks are observed in the range from 420 to 470 K, which are magnified in Fig. 2(b). Martensite transformation is thought to be responsible for these peaks. No peaks are found for the sample prepared at 1723 K. Some researchers reported that the $Cu_{50}Zr_{50}$-based alloys can exhibit a martensite transformation when cooled quickly to a temperature below 440 K,[24] which is confirmed in this work. Furthermore, it suggests that the sample prepared at 1723 K is amorphous. The result is supported by the calculation of crystallization enthalpy for these samples. The magnitude of crystallization enthalpy is thought to be a function of the content of the amorphous phase. From Fig. 2 and Table I, we can see the value of the enthalpy of crystallization increases with increasing casting temperature. The content of the crystalline phase in the amorphous matrix is calculated with the expression of "$1-E_{simple}/E_{reference}$", where E_{sample} and $E_{reference}$ are the enthalpy of the sample and the reference, respectively. The reference is fully amorphous. The calculation method is applicable in the present work as the compositions of the amorphous matrix prepared under different casting temperatures are similar. We used energy dispersive x-ray spectroscopy (EDS) to check the compositions of the amorphous phase and crystalline phases, which are $Zr_{46.29}Cu_{49.31}Ti_{2.49}Y_{1.91}$ and $Zr_{46.55}Cu_{48.82}Ti_{2.58}Y_{2.05}$ (in atomic percentage), respectively. Herein, we take the 2-mm-diameter sample prepared under 1723 K as the reference material. The content of the crystalline phase of the samples prepared at the other two casting temperatures is calculated, which is 25% for 1523 K and 32% for 1323 K. It can be seen that the content of crystalline phases fall with increasing casting temperature, and when the casting temperature reaches 1723 K no crystalline phases are formed. From these results, one may conclude that a high casting temperature would enhance GFA. It also implies that adjusting the amount and size of the crystalline phase in the BMGCs by controlling the casting temperature is possible. It is beneficial to the understanding of the relationship of microstructures to the mechanical properties for BMGCs and monolithic BMGs.

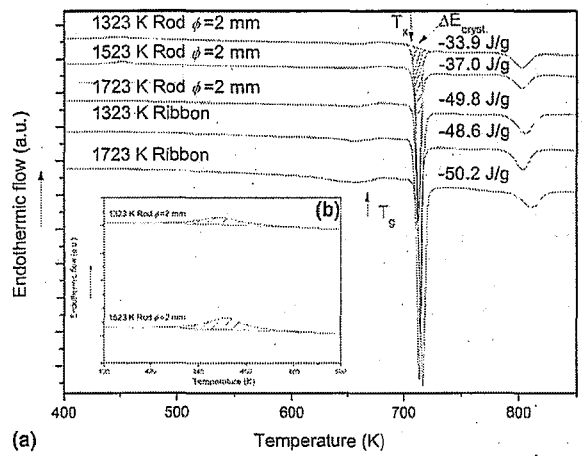

FIG. 2. (a) DSC scanning of as-cast rods with 2 mm diameter of $Cu_{50}Zr_{45.5}Ti_{2.5}Y_2$ alloy prepared under different casting temperatures. For comparison, the DSC curve of ribbon quenched at 1723 K is listed together. The inset in (b) is a high magnification of the rectangle in (a).

TABLE I. Thermal parameters of the samples prepared under different casting temperatures obtained by DSC measurement at a heating rate of 20 K/min.

	T_1 (K)	T_2 (K)	$\Delta E_{m,t.}$ (J/g)	T_g (K)	T_x (K)	$\Delta E_{cryst.}$ (J/g)
1323 K Φ = 2 mm	437	466	2.6	660	709	−33.9
1523 K Φ = 2 mm	435	461	2.0	663	709	−37.0
1723 K Φ = 2 mm	...	...	...	663	710	−49.8
1323 K ribbon	...	...	...	666	709	−48.6
1723 K ribbon	...	...	...	666	712	−50.2

T_1, T_2, and $\Delta E_{m,t}$ are onset temperature, finishing temperature, and heat of martensite transformation. T_g, T_x, and $\Delta E_{cryst.}$ are glass transition temperature, onset crystallization temperature, and the enthalpy of crystallization.

The morphologies of the crystalline phases in different samples are shown in Fig. 3. Figures 3(a)–3(c) correspond to 2-mm-diameter samples prepared at 1323, 1523, and 1723 K, respectively. When the casting temperatures are 1323 and 1523 K, the crystals are observed in the form of spheres. Most of crystalline phases are aggregated together, which may be due to the inhomogeneous distribution of the cooling rate along the radial direction during casting. When the casting temperature elevates to 1723 K, no crystals are observed, as seen in Fig. 3(c). The amount of the crystalline phases in the samples with different casting temperatures is consistent with the XRD and DSC measurements. These results also support the conclusion that increasing the casting temperature enhances GFA of the alloy.

It is generally accepted that the introduction of the second phase, such as fiber, dendrite, particle, etc., into the amorphous matrix helps to improve the properties of BMGs,[8–12] especially plasticity, which is one of the principal restraints for BMGs' commercial applications. In the present work, we also examined the effect of precipitated CuZr phases on mechanical properties of the samples using nanoindentation tests and compression tests.

The nanoindentation test was used to investigate the properties of CuZr phases and the amorphous matrix, and the results are shown in Fig. 4. The specimen is a 2-mm-diameter as-cast rod prepared at 1523 K. As mentioned previously, the composition of the crystalline phase is nearly the same as that of the amorphous matrix. Accordingly, the results shown in Fig. 4 are also suitable for specimens with different casting temperatures. Figure 4(a)

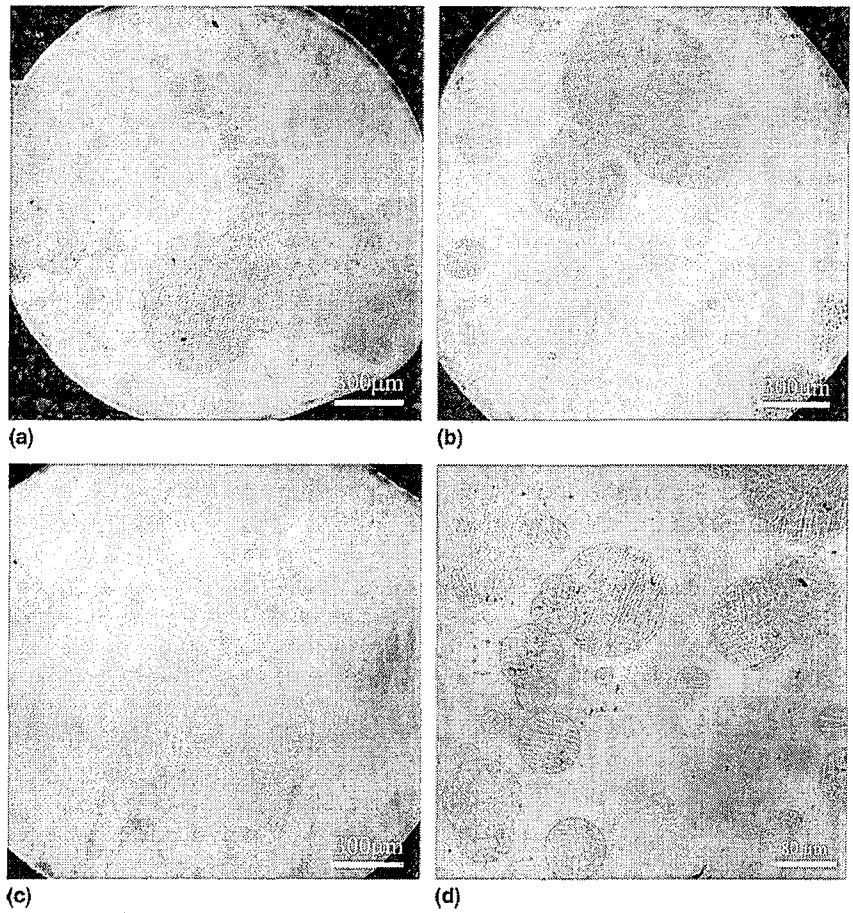

FIG. 3. Optical images of as-cast rods with different diameters in $Cu_{50}Zr_{45.5}Ti_{2.5}Y_2$ alloy prepared under different casting temperatures: (a) 2 mm, 1323 K, (b) 2 mm, 1523 K, (c) 2 mm, 1723 K, and (d) 1.5 mm, 1323 K.

shows the load–depth curves under different maximum loads. The area enveloped by the load–depth curves and the horizontal axis is larger for CuZr phases than for the amorphous matrix under different maximum loads, indicating that CuZr phases can accommodate more plastic deformation in the localized zone than the amorphous matrix. In addition, the CuZr phases are slightly softer than the amorphous matrix, which is indicated by the hardness in Fig. 4(c), 6.1 GPa for the CuZr phases and 6.3 GPa for the amorphous matrix. Figure 4(b) shows that the CuZr phases have slightly higher Young's modulus than the amorphous matrix.

Mechanical properties of samples prepared under different casting temperatures were also studied using compression tests. The typical true stress–strain curves for the samples are shown in Fig. 5. The samples prepared at 1723 K yielded at about 1600 MPa and immediately fractured at 1770 MPa with little plastic deformation (about 0.5%). For samples prepared at 1323 and 1523 K, the yield strength falls to about 1100 and 1220 MPa, respectively, followed by obvious work hardening. The materials fail at 1770 and 1820 MPa, respectively, with plastic deformation of about 5% and 7% at fracture. Similar phenomena were reported in other CuZr-[19–23,25–27] and TiCu-[26] based amorphous alloys. Multiple shear bands are believed to soften BMG materials.[28] Figure 5 also shows the compressive stress–strain curve of the 3-mm-diameter as-cast sample, which consists of CuZr phases, as shown in Fig. 1. This sample exhibits extraordinary work hardening, yielding at about 460 MPa and rapidly increasing to about 1750 MPa with about 6% plastic deformation. The improvement of the plasticity of Cu–Zr–Ti–Y metallic glass was further confirmed by observing the density of shear bands on the lateral surfaces of the specimens prepared at 1323, 1523, and 1723 K. As shown in Fig. 6, profuse shear bands were seen on the samples prepared at 1323 and 1523 K, which make the materials experience a lot of plastic deformation without failure. Contrarily, rare shear bands were observed on the samples prepared at 1723 K, indicating that the specimen deformed in a brittle way. These results are consistent with Fig. 5. Figures 6(d), 6(e), and 6(f) are the fracture surfaces of the composite, full-amorphous and almost full-CuZr-phase samples,

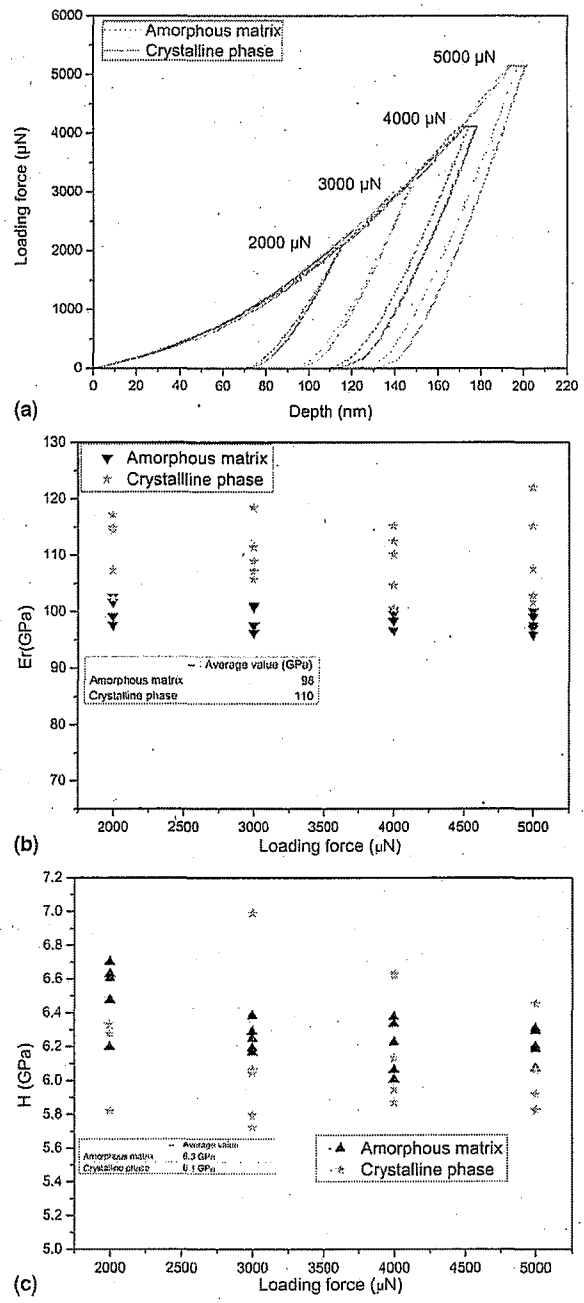

FIG. 4. (a) Load–depth curves, (b) Young's modulus, and (c) hardness of as-cast rod with 2 mm diameter prepared under 1523 K in $Cu_{50}Zr_{45.5}Ti_{2.5}Y_2$ alloy, obtained by nanoindentation tests under different maximum loads.

respectively. Some disturbance on the vein-patterns of the samples prepared at 1523 K marked by the ellipses in Fig. 6(d) reveal that the occurrence of the CuZr phase can obstruct the development of vein-patterns. It also means that the CuZr phase can block the propagation of shear bands, leading to the production of multiple shear bands.[19–23,25–28] The deformability of the CuZr phase (Fig. 5) will increase the resistance of the plastic deformation of the samples prepared at the relatively lower

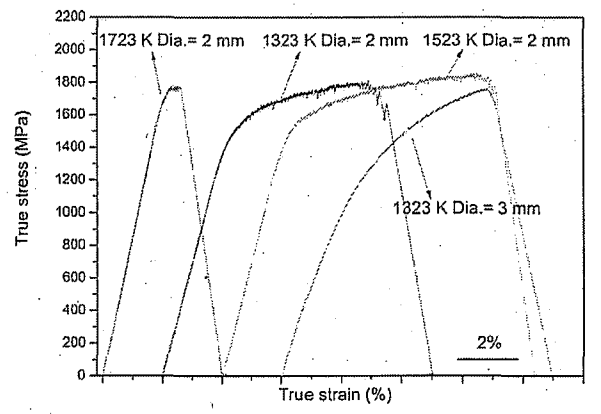

FIG. 5. Typical true stress–strain curves of as-cast rods with different diameters and different casting temperatures in $Cu_{50}Zr_{45.5}Ti_{2.5}Y_2$ alloy, obtained by uniaxial compression tests at the strain rate of $2 \times 10^{-4}s^{-1}$. The ratio of length to diameter of all the specimens is 2:1.

casting temperature. As a result, we considered that CuZr phases formed at the lower casting temperatures of 1323 and 1523 K significantly improve mechanical properties of BMGs and are responsible for their work hardenability.

IV. DISCUSSION

Casting temperature has a large influence on the GFA of the alloy, as shown in Fig. 1. Generally, one always correlates glass formation to nucleation and growth of crystals.[8–10,29] To obtain high GFA, techniques avoiding the crystallization in the melt is highly desirable. From Fig. 1, we identified that the primary competing crystalline phase against glass formation is CuZr phases in the present alloy. To better understand the crystallization process of CuZr phases, we observed the morphology of CuZr phases at higher magnification, as shown in Fig. 3(d) and compared with Figs. 3(a) and 3(b). The crystals are heterogeneously distributed in the amorphous matrix whether on a macroscopic [Figs. 3(a) and 3(b)] or microscopic [Fig. 3(d)] scale. This sheds light on the formation mechanism of CuZr phases. Heterogeneous distribution of CuZr phases may be attributed to the following two reasons. First, the inhomogeneous distribution of the cooling rate along the radial direction, as mentioned previously, leads to the macroscopic inhomogeneity. The second reason is the occurrence of heterogeneity in the melt,[4,30–32] which induces preferential nucleation and growth in some sites. These nuclei grow in the form of spheres, which is different from the growth mechanism of dendrites. With crystallization proceeding, the aggregation occurs, as marked in Fig. 3(d). This accelerates the crystallization, which leads to the morphology of crystals shown in Figs. 3(a) and 3(b).

The pre-existing nuclei in the melt can be from two possible sources. One is the local ordering cluster, which is suggested to exist in the melt by previous

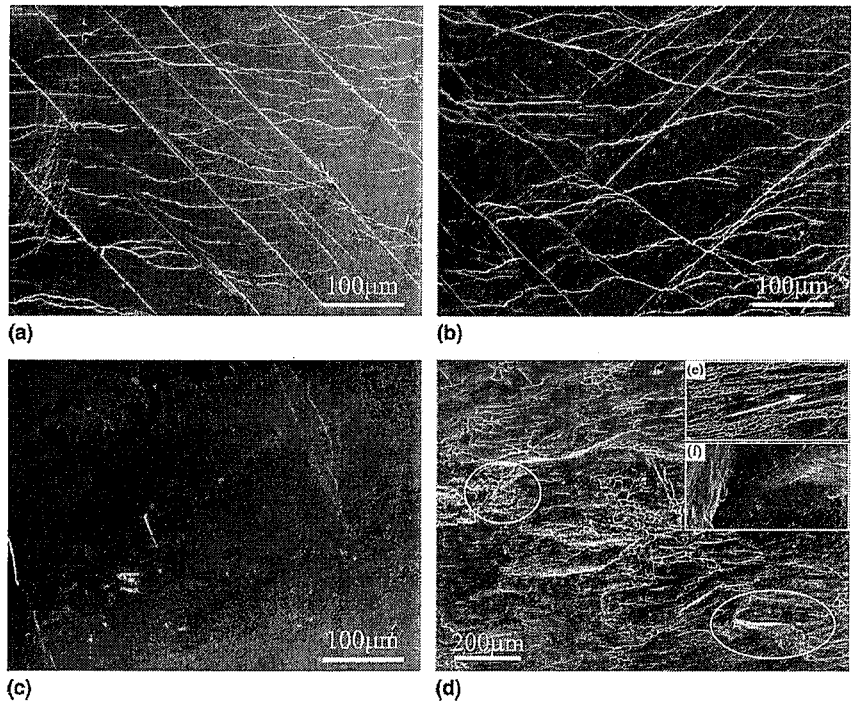

FIG. 6. SEM images (a)–(c) corresponding to the lateral surfaces of fractured samples prepared under 1323, 1523, and 1723 K, respectively; (d, e) corresponding to the fracture surface of the samples prepared under 1523 and 1723 K; (f) corresponding to the fracture surface of almost full-CuZr phase sample with 3 mm in diameter prepared at 1323 K.

literature.[4,30–32] The other is the surviving crystals, which can melt at ultrahigh temperature. Both are thought to be metastable and can gradually dissipate with increasing temperature.[4,30–32] For the local ordering cluster, its effectiveness as a nucleation site is closely correlated to the temperature. At a temperature far below the critical temperature, the heterogeneities were reported to remain in the melt for a long time. Conversely, when the temperature is over the critical temperature, the heterogeneities simultaneously dissipate. The critical temperature of this transformation was proposed to be about 1.4 T_m (melting temperature of the alloy).[3,4,30–32] The surviving crystal might be the Cu_5Zr phase in the present alloy. In $Cu_{50}Zr_{50}$ alloy, metastable eutectic involving Cu_5Zr and Zr is suggested to be responsible for its high GFA.[33] Cu_5Zr is primarily precipitated when annealing the amorphous $Cu_{50}Zr_{50}$ alloy. The similar result was reported in $Cu_{46}Zr_{54}$ alloy by Wang et al.[34] Other papers reported the discovery of nanoscale Cu_5Zr in the rapidly solidified $Cu_{50}Zr_{50}$[35] and Zr–Cu–Ni–Al alloys.[36] In this work, the investigated alloy is $Cu_{50}Zr_{50}$-based. It is possible to form a small amount of tiny Cu_5Zr particles in the rapidly cooled master ingot obtained by arc melting. According to the Tournier's theory,[37] tiny particles survive at a temperature of 1388 K, which is only about 1.2 $T_{m,\ Cu5Zr}$ ($T_{m,\ Cu5Zr}$ is the melting temperature of Cu_5Zr.) when the master ingot is remelted to prepare the samples using copper mold casting. The survival of these tiny crystals would affect the microstructures of the resultant as-cast samples. As a result, the occurrence of heterogeneity in the melt depends on the casting temperature. When the casting temperature is high (1723 K in the present work), heterogeneity would disappear in the melt and GFA will be enhanced. It is consistent with the results we previously reported that the enhancement of thermal stability was observed in the amorphous alloys prepared at high casting temperature. While the samples cast at low casting temperatures (1323 and 1523 K in the present work), some crystals will precipitate.

Although the heterogeneity surviving in the melt under low casting temperature deteriorates GFA of the alloy, the crystal phases grown up from those heterogeneity improve the mechanical properties of BMGs,[14] as shown in Fig. 5. The samples with homogeneous amorphous structure obtained by high casting temperature casting exhibit brittleness, like most of the BMGs. The CuZr phases formed in the samples prepared at low casting temperatures are softer and more ductile than the amorphous matrix. Under loading, the CuZr phases will undergo plastic deformation at a relatively low stress level while the amorphous matrix remains elastic. This kind of inconsistency of deformation behaviors between the amorphous matrix and CuZr phases leads to stress concentration on the interface. It is generally accepted that the in situ formed CuZr crystals are well bonded with the glassy matrix, which avoids the initiation of the cracks on the interface. To keep the

consistency of deformation behaviors between the amorphous matrix and CuZr phases, shear bands would be initiated in the amorphous matrix under further loading. This leads to the loss of yield strength in the materials, which is shown in Fig. 5. However, multiple shear bands initiating in the amorphous matrix can accommodate much plastic deformation, contributing to the improvement of plasticity of the materials (Fig. 4).

In general, GFA and property of BMGs are closely related to their solidification conditions.[3,14,15] Controlling solidification conditions, for example casting temperatures in the present work, not only enhances GFA of the alloy, but also improves mechanical properties of BMGs by introducing structural heterogeneity on a macro- or nanoscale.[14] Understanding the relationship between solidification conditions and properties of BMGs would be significant and beneficial to promote BMGs' applications.

V. CONCLUSION

The influence of casting temperature on microstructures and mechanical properties of $Cu_{50}Zr_{45.5}Ti_{2.5}Y_2$ alloy prepared using copper mold casting were investigated in the present work. This leads us to draw the following conclusions:

(1) With the increase of casting temperature, GFA of the alloy is enhanced. Under the casting temperature of 1723 K, full amorphous sample was successfully made at a size of 2 mm in diameter in the $Cu_{50}Zr_{45.5}Ti_{2.5}Y_2$ alloy. Under the lower casting temperatures, CuZr phases were primarily precipitated in the alloy. It is thought to be attributed to the crystals or clusters surviving in the melt.

(2) The introduction of the CuZr phase by controlling the casting temperature effectively improves the plasticity of Cu–Zr–Ti–Y metallic glass. The amount of CuZr phases is related to the casting temperature. Mechanical tests indicate that CuZr phases are softer and more ductile than the amorphous matrix. Under loading, CuZr phases induce the initiation of multiple shear bands, leading to large improvement in the plasticity of the materials.

(3) Through the comparison of the deformation behaviors between CuZr phases, amorphous matrix, and composite work hardenability, the composite exhibited in the compression tests is thought to be attributed to the precipitated CuZr phases instead of the amorphous matrix.

ACKNOWLEDGMENTS

Y.Q. Wu from the University of Queensland is appreciated for the assistance of nanoindentation tests. The authors gratefully acknowledge the financial support from the Ministry of Science and Technology of China (Grant Nos. 2006CB605201 and 2010CB731602) and the National Natural Science Foundation of China (Grant Nos. 50825402 and 50731005).

REFERENCES

1. D.R. Askeland and P.P. Phule: *The Science and Engineering of Materials*, 4th ed. (Tsinghua University Press, Beijing, China, 2004), pp. 5, 27.
2. G.I. Eskin: *Ultrasonic Treatment of Light Alloy Melts* (CRC Press, Boca Raton, FL, 1998).
3. V. Manov, P. Popel, E. Brook-Levinson, V. Molokanov, M. Calvo-Dahlborg, U Dahlborg, V. Sidorov, L. Son, and Y. Tarakanov: Influence of the treatment of melt on the properties of amorphous materials: Ribbons, bulks and glass coated microwires. *Mater. Sci. Eng., A* **304–306,** 54 (2001).
4. P.S. Popel, O.A. Chikova, and V.M. Matveev: Metastable colloidal states of liquid metallic solutions. *High Temp. Mater. Processes* **14,** 219 (1995).
5. P.S. Popel, M. Calvo-Dahlborg, and U. Dahlborg: Metastable microheterogeneity of melts in eutectic and monotectic systems and its influence on the properties of the solidified alloy. *J. Non-Cryst. Solids* **353,** 3243 (2007).
6. W. Klement, R.H. Willens, and P. Duwez: Non-crystalline structure in solidified gold-silicon alloys. *Nature* **187,** 869 (1960).
7. C.J. Byrne and M. Eldrup: Materials science: Bulk metallic glasses. *Science* **321,** 502 (2008).
8. W.L. Johnson: Bulk glass-forming metallic alloys: Science and technology. *MRS Bull.* **24,** 42 (1999).
9. W.H. Wang, C. Dong, and C.H. Shek: Bulk metallic glasses. *Mater. Sci. Eng., R* **44,** 45 (2004).
10. Y. Li, S.J. Poon, G.J. Shiflet, J. Xu, D.H. Kim, and J.F. Löffler: Formation of bulk metallic glasses and their composites. *MRS Bull.* **32,** 624 (2007).
11. H. Choi-Yim and W.L. Johnson: Bulk metallic glass matrix composites. *Appl. Phys. Lett.* **71,** 3808 (1997).
12. R.D. Conner, R.B. Dandliker, and W.L. Johnson: Mechanical properties of tungsten and steel fiber reinforced $Zr_{41.25}Ti_{13.75}Cu_{12.5}Ni_{10}Be_{22.5}$ metallic glass matrix composites. *Acta Mater.* **46,** 6089 (1998).
13. J. Shen, Y.J. Huang, and J.F. Sun: Plasticity of a TiCu-based bulk metallic glass: Effect of cooling rate. *J. Mater. Res.* **22,** 3067 (2007).
14. Z.W. Zhu, S.J. Zheng, H.F. Zhang, B.Z. Ding, Z.Q. Hu, P.K. Liaw, Y.D. Wang, and Y. Ren: Plasticity of bulk metallic glasses improved by controlling the solidification condition. *J. Mater. Res.* **23,** 941 (2008).
15. Z.W. Zhu, H.F. Zhang, H. Wang, B.Z. Ding, and Z.Q. Hu: The influence of casting temperature on the thermal stability of Cu- and Zr-based MGs: Theoretic analysis and experiments. *J. Mater. Res.* **23,** 2714 (2008).
16. A. Inoue, W. Zhang, and J. Saida: Synthesis and fundamental properties of Cu-based bulk glassy alloys in binary and multicomponent systems. *Mater. Trans.* **45,** 1153 (2004).
17. A. Inoue, W. Zhang, T. Zhang, and K. Kurosaka: Thermal and mechanical properties of Cu-based Cu–Zr–Ti bulk glassy alloys. *Mater. Trans.* **42,** 1149 (2001).
18. Q.S. Zhang, W. Zhang, G.Q. Xie, K.S. Nakayama, H. Kimura, and A. Inoue: Formation of bulk metallic glass in situ composites in $Cu_{50}Zr_{45}Ti_5$ alloy. *J. Alloys Compd.* **431,** 236 (2007).
19. Q. Zhang, H. Zhang, Z. Zhu, and Z. Hu: Formation of high strength in-situ bulk metallic glass composite with enhanced plasticity in $Cu_{50}Zr_{47.5}Ti_{2.5}$ alloy. *Mater. Trans.* **46,** 730 (2005).

20. Y.F. Sun, B.C. Wei, Y.R. Wang, W.H. Li, T.L. Cheung, and C.H. Shek: Plasticity-improved Zr–Cu–Al bulk metallic glass matrix composites containing martensite phase. *Appl. Phys. Lett.* **87,** 051905 (2005).
21. F. Jiang, Z.B. Zhang, L. He, J. Sun, H. Zhang, and Z.F. Zhang: The effect of primary crystallizing phases on mechanical properties of $Cu_{46}Zr_{47}Al_7$ bulk metallic glass composites. *J. Mater. Res.* **21,** 8 (2006).
22. S. Pauly, J. Das, C. Duhamel, and J. Eckert: Martensite formation in a ductile $Cu_{47.5}Zr_{47.5}Al_5$ bulk metallic glass composite. *Adv. Eng. Mater.* **9,** 487 (2007).
23. J. Das, K.B. Kim, W. Xu, B.C. Wei, Z.F. Zhang, W.H. Wang, S. Yi, and J. Eckert: Ductile metallic glasses in supercooled martensitic alloys. *Mater. Trans.* **47,** 2606 (2006).
24. E.M. Carvalho and I.R. Harris: Constitutional and structural studies of the intermetallic phase, ZrCu. *J. Mater. Sci.* **15,** 1224 (1980).
25. Z.W. Zhu, H.F. Zhang, W.S. Sun, B.Z. Ding, and Z.Q. Hu: Processing of bulk metallic glasses with high strength and large compressive plasticity in $Cu_{50}Zr_{50}$. *Scr. Mater.* **54,** 1145 (2006).
26. K.B. Kim, J. Das, S. Venkataraman, S. Yi, and J. Eckert: Work hardening ability of ductile $Ti_{45}Cu_{40}Ni_{7.5}Zr_5Sn_{2.5}$ and $Cu_{47.5}Zr_{47.5}Al_5$ bulk metallic glasses. *Appl. Phys. Lett.* **89,** 071908 (2006).
27. J. Das, M.B. Tang, K.B. Kim, R. Theissmann, F. Baier, W.H. Wang, and J. Eckert: "Work-hardenable" ductile bulk metallic glass. *Phys. Rev. Lett.* **94,** 205501 (2005).
28. H. Bei, S. Xie, and E.P. George: Softening caused by profuse shear banding in a bulk metallic glass. *Phys. Rev. Lett.* **96,** 105503 (2006).
29. K.F. Kelton: Crystal nucleation in liquids and glasses. *Solid State Phys.* **45,** 75 (1991).
30. W. Hoyer and R. Jodicke: Short-range and medium-range order in liquid Au–Ge alloys. *J. Non-Cryst. Solids* **192–193,** 102 (1995).
31. K.F. Kelton, G.W. Lee, A.K. Gangopadhyay, R.W. Hyers, T.J. Rathz, J.R. Rogers, M.B. Robinson, and D.S. Robinson: First x-ray scattering studies on electrostatically levitated metallic liquids: Demonstrated influence of local icosahedral order on the nucleation barrier. *Phys. Rev. Lett.* **90,** 195504 (2003).
32. H. Jónsson and H.C. Andersen: Icosahedral ordering in the Lennard-Jones liquid and glass. *Phys. Rev. Lett.* **60,** 2295 (1988).
33. W.H. Wang, J.J. Lewandowski, and A.L. Greer: Understanding the glass-forming ability of $Cu_{50}Zr_{50}$ alloys in terms of a metastable eutectic. *J. Mater. Res.* **20,** 2307 (2005).
34. H.R. Wang, Y.F. Ye, Z.Q. Shi, X.Y. Teng, and G.H. Min: Crystallization processes in amorphous $Zr_{54}Cu_{46}$ alloy. *J. Non-Cryst. Solids* **311,** 36 (2002).
35. A. Inoue, W. Zhang, T. Tsurui, A.R. Yavari, and A.L. Greer: Unusual room-temperature compressive plasticity in nanocrystal-toughened bulk copper-zirconium glass. *Philos. Mag. Lett.* **85,** 221 (2005).
36. T.A.M. Aboki, F. Brisset, J.P. Souron, A. Dezellus, and P. Plaindoux: Microstructure studies of $Zr_{65}Cu_{17.5}Al_{7.5}Ni_{10}$ and $Zr_{65}Cu_{15}Al_{10}Ni_{10}$ glass forming alloys: Phase morphologies and undercooled melt solidification. *Intermetallics* **16,** 615 (2008).
37. R.F. Tournier: Presence of intrinsic growth nuclei in overheated and undercooled liquid elements. *Physica B* **392,** 79 (2007).